A Pre-trained Deep Potential Model for Sulfide Solid Electrolytes with Broad Coverage and High Accuracy

Ruoyu Wang[1,2,3,*], Mingyu Guo[4,5,*], Yuxiang Gao[1,2], Xiaoxu Wang[4,6], Yuzhi Zhang[4,6], Bin Deng[4], Mengchao Shi[3,4,§], Linfeng Zhang[4,6,‡] and Zhicheng Zhong[1,2,3,†]

[1]School of Artificial Intelligence and Data Science, University of Science and Technology of China, Hefei 230026, China

[2]Suzhou Institute for Advanced Research, University of Science and Technology of China, Suzhou 215123, China

[3]Suzhou Lab, Suzhou 215123, China

[4]DP Technology, Beijing 10080, China

[5]School of Chemistry, Sun Yat-sen University, Guangzhou 510006, China

[6]AI for Science Institute, Beijing 10080, China

[*]The two authors contributed equally to this work.

[§]shimengchao@dp.tech

[‡]linfeng.zhang.zlf@gmail.com

[†]zczhong@ustc.edu.cn

I. SUPPLEMENTARY RESULTS

A. Benchmark test

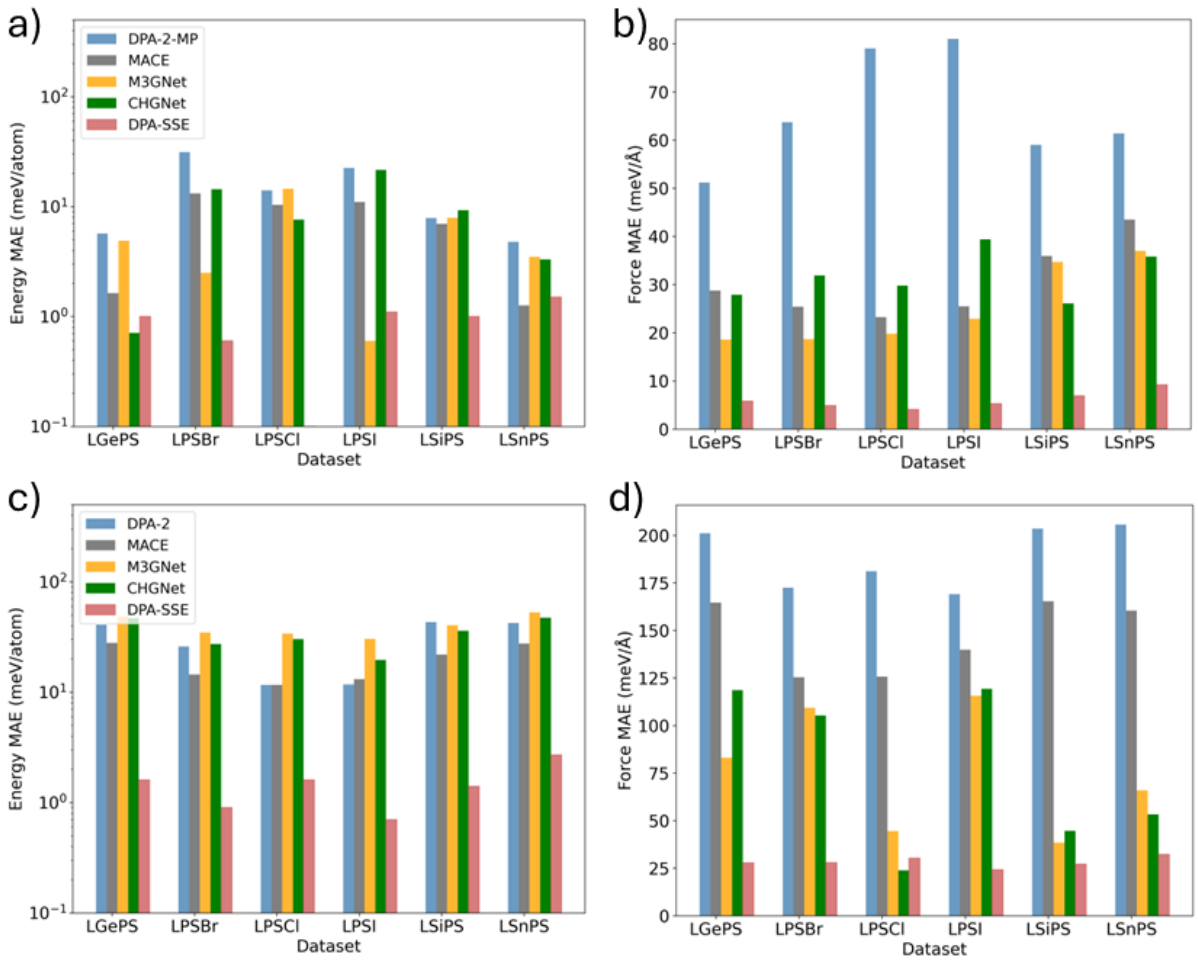

FIG. S1. The energy and force prediction error of DPA-SSE and other universal force fields on near-equilibrium configurations of various sulfide electrolytes. The test sets are produced by running DeePMD simulation at 50 K for 10 steps.

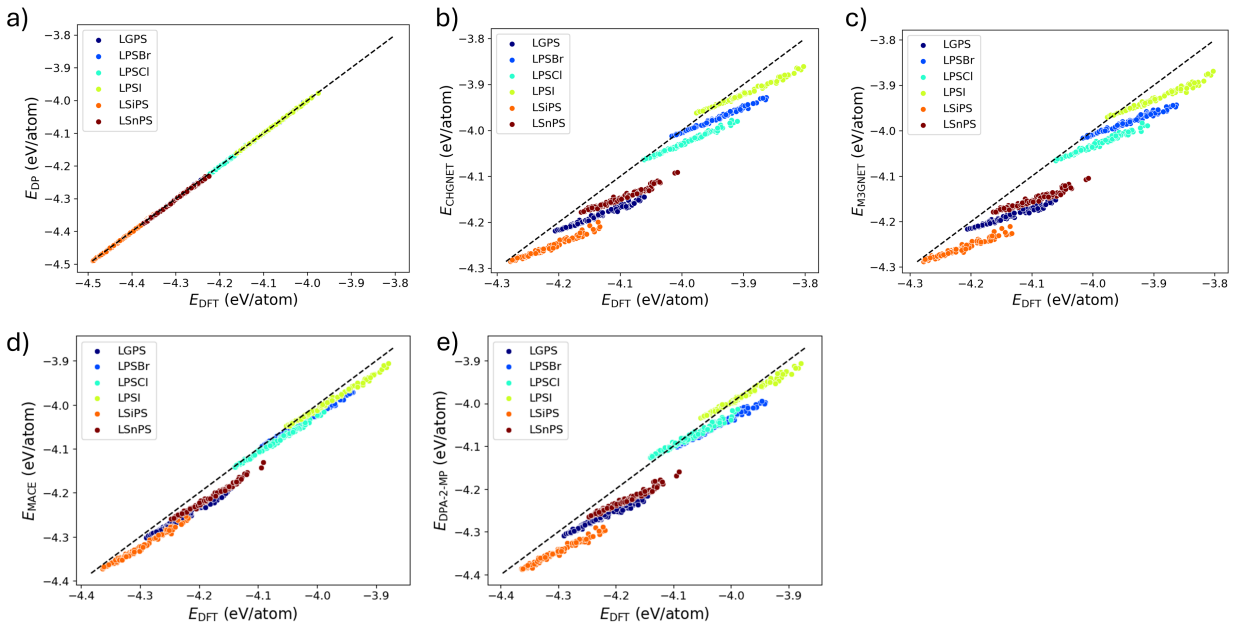

FIG. S2. The energy prediction error of **a)** DPA-SSE, **b)** CHGNet, **c)** M3GNet, **d)** MACE and **e)** DPA-2-MP on a heating DeePMD trajectory from 150 to 1150 K.

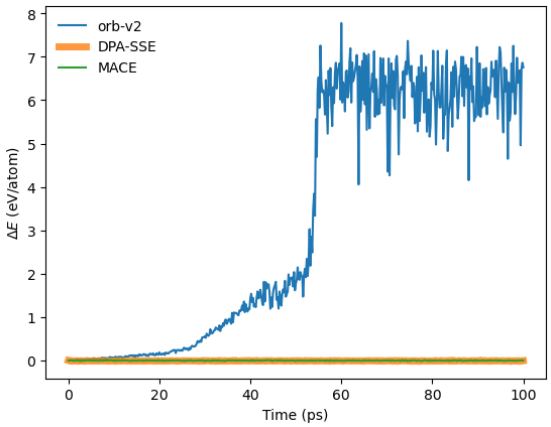

FIG. S3. Potential energy drift in an NVE simulation of LGPS with ORB, MACE and DPA-SSE models. The simulation systems are first heated to 500 K with NVT simulation. The ORB model is not conservative, *i.e.*, forces are not derivatives of potential energy. Consequently, significant energy drift occurs after long NVE simulations, whereas the energy conservation should have been ensured.

B. Structural relaxation

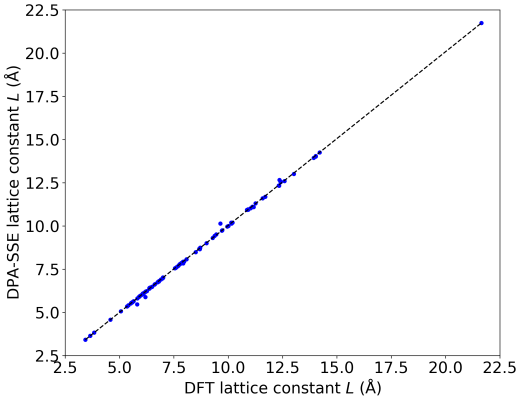

FIG. S4. Structural relaxation. The relaxed lattice constant of the 41 compounds covered in the training set as predicted by DPA-SSE and DFT calculation.

C. Thermal stability

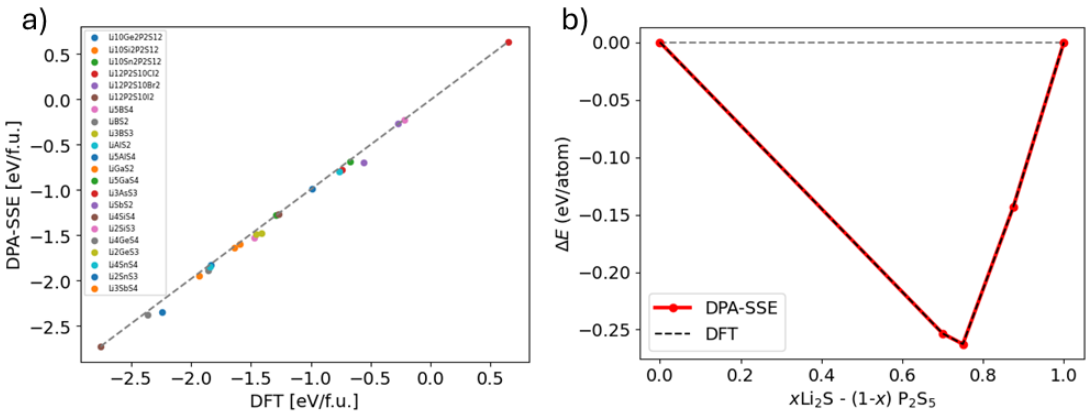

FIG. S5. Formation energies benchmark. (a)The decomposition energy of 22 compounds as predicted by DPA-SSE and DFT calculation. (b)The formation energy of Li_2S-P_2S_5 pseudo-binary system as a function of composition.

D. Model fine-tuning

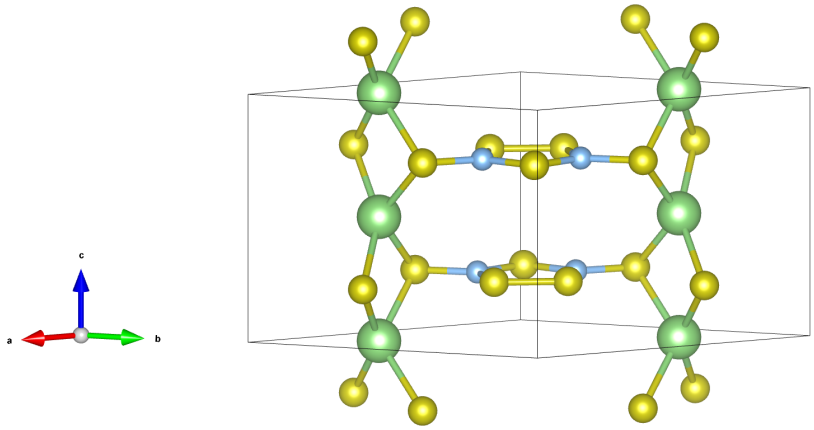

FIG. S6. The crystal structure of LBS mp-29410 compounds. The Li, B and S atoms are represented by green, blue and yellow colors, respectively.

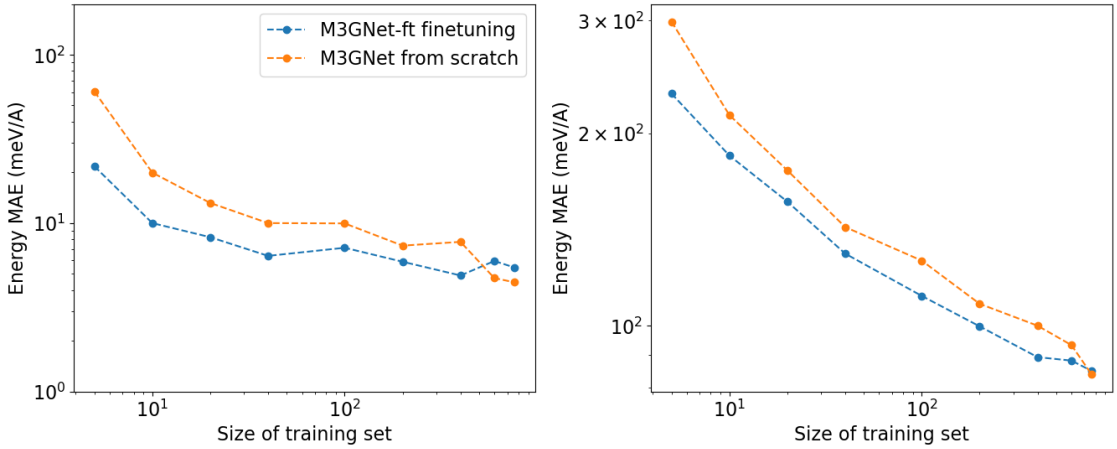

FIG. S7. Energy and force learning rate of randomly initialized M3GNet model and pre-trained M3GNet model fine-tuned with DPA-SSE dataset, on the continuous learning task of LBS system shown in Figure S6. Both models are trained for 133 epochs with identical training parameters.

E. Ionic transport simulation

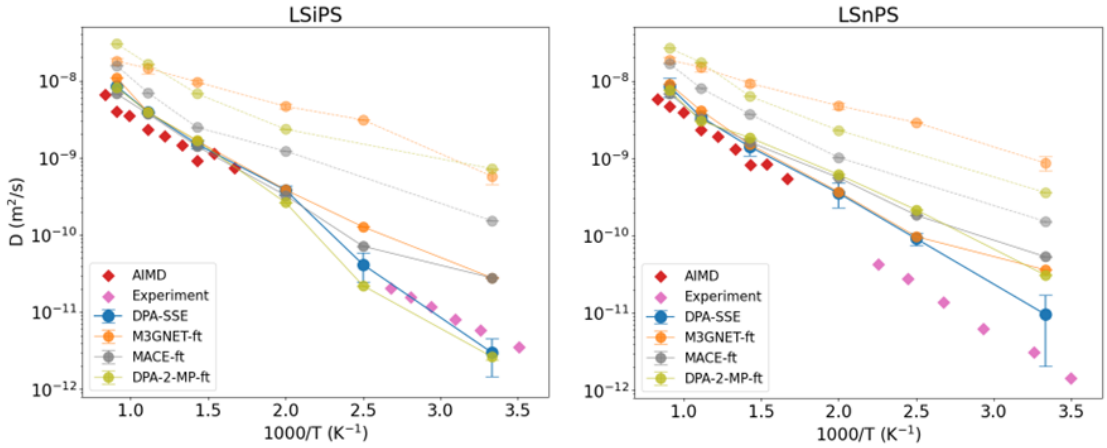

FIG. S8. The experimental and calculated diffusion coefficient of a) $Li_{10}SiP_2S_{12}$ and b) $Li_{10}SnP_2S_{12}$ solid electrolyte.

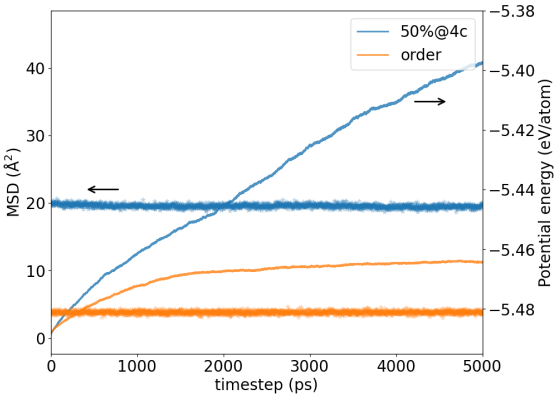

FIG. S9. The time evolution of room temperature mean square displacement (MSD) and potential energy of Li_6PS_5I solid electrolytes.

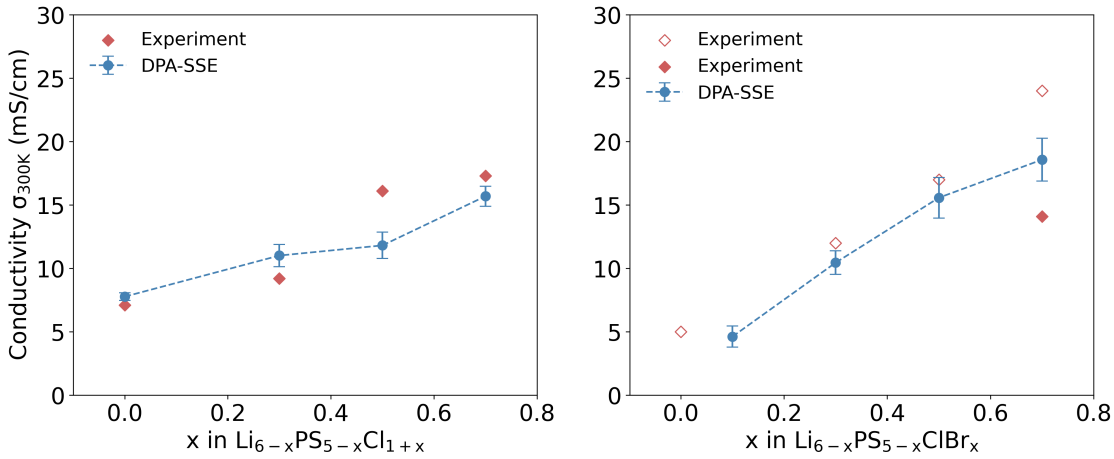

FIG. S10. Calculated room temperature lithium-ion conductivity of Li_6PS_5Cl solid electrolyte as a function of excess (a) Cl[1] and (b) Br[2, 3] doping. For comparison, experiment results are also listed.

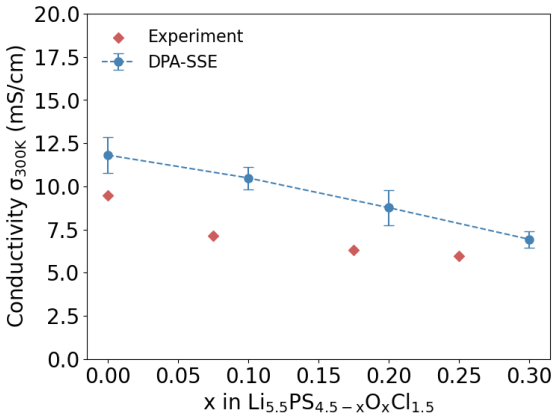

FIG. S11. Calculated room temperature lithium-ion conductivity of $Li_{5.5}PS_{4.5-x}O_xCl_{1.5}$ solid electrolyte as a function of O doping, which help improve moisture stability critical to industrial application. For comparison, experimental measurements are also presented[4].

F. Model distillation

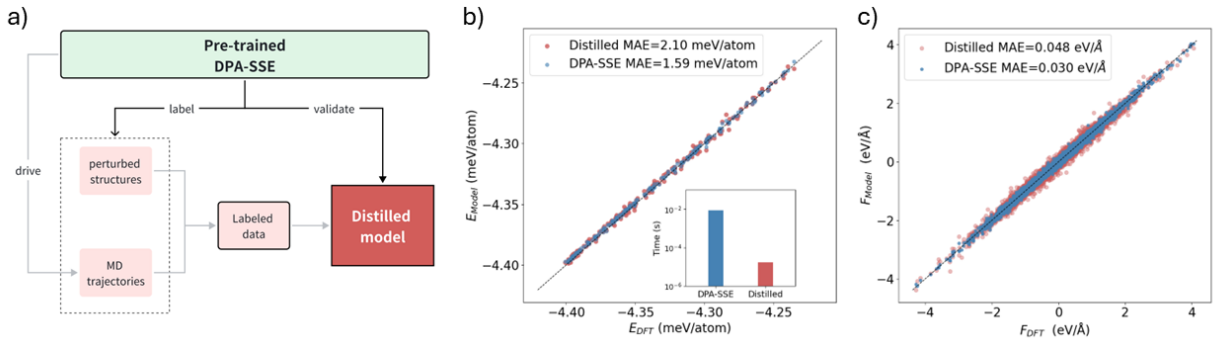

FIG. S12. **Model distillation for efficient dynamic simulation.** a) The schematic of the distillation process. The b) energy and c) force prediction for the pre-trained and distilled model on an AIMD trajectory of LGPS at 900 K. The inset of b) compares the efficiency of two models.

[1] Sawankumar V. Patel, Swastika Banerjee, Haoyu Liu, Pengbo Wang, Po-Hsiu Chien, Xuyong Feng, Jue Liu, Shyue Ping Ong, and Yan-Yan Hu. Tunable Lithium-Ion Transport in Mixed-Halide Argyrodites $Li_{6-x}PS_{5-x}ClBr_x$: An Unusual Compositional Space. *Chemistry of Materials*, 33(4):1435–1443, February 2021.

[2] Yu Liu, Han Su, Yu Zhong, Matthew Zheng, Yang Hu, Feipeng Zhao, Jung Tae Kim, Yingjie Gao, Jing Luo, Xiaoting Lin, Jiangping Tu, and Xueliang Sun. Inhibiting Dendrites by Uniformizing Microstructure of Superionic Lithium Argyrodites for All-Solid-State Lithium Metal Batteries. *Advanced Energy Materials*, 14(31):2400783, August 2024.

[3] Xuyong Feng, Po-Hsiu Chien, Yan Wang, Sawankumar Patel, Pengbo Wang, Haoyu Liu, Marcello Immediato-Scuotto, and Yan-Yan Hu. Enhanced ion conduction by enforcing structural disorder in Li-deficient argyrodites Li6xPS5xCl1+x. *Energy Storage Materials*, 30:67–73, September 2020.

[4] Linfeng Peng, Shaoqing Chen, Chuang Yu, Chaochao Wei, Cong Liao, Zhongkai Wu, Hsing-Lin Wang, Shijie Cheng, and Jia Xie. Enhancing Moisture and Electrochemical Stability of the Li5.5PS4.5Cl1.5 Electrolyte by Oxygen Doping. *ACS Applied Materials & Interfaces*, 14(3):4179–4185, January 2022. Publisher: American Chemical Society.